[GC]Target-Oriented Parameters for Curvature Attributes Computation*

Lee Hunt[3], Bahaa Beshry[2], Satinder Chopra[1], and Cole Webster[2]

Search and Discovery Article #42146 (2017)
Posted October 30, 2017

*Adapted from the Geophysical Corner column, prepared by the authors, in AAPG Explorer, October, 2017. Editor of Geophysical Corner is Satinder Chopra (schopra@arcis.com). Managing Editor of AAPG Explorer is Brian Ervin.

[1]Arcis Seismic Solutions, TGS, Calgary, Canada (schopra@arcis.com)
[2]Jupiter Resources, Calgary, Canada
[3]Retired geophysicist

General Statement

Curvature has long been used by geologists to predict the density of natural fractures from outcrop. Sand box experiments show that correlations between curvature and strain can be significant, which is supportive of the curvature-strain-natural fractures supposition inherent in the use of curvature to predict natural fractures. Seismic horizon-based curvature estimates have been shown to be potentially effective in the same manner as that of geologic map approaches. This was followed by volumetric seismic curvature, which has largely replaced horizon-based curvature estimates perhaps due to the elimination of picking a horizon in data not well suited to horizon picking, or not having a pickable horizon in our zone of interest.

The first author and others have found statistically significant correlations between volumetric most-positive curvature and natural fracture density indicated from high-resolution image log data along horizontal wells. One of the methods of computing seismic volumetric curvature attribute involves Fourier filtering, and has gained widespread acceptance. There are other methods for generation and filtering of curvature that are available in our industry. We examine the impact of specific curvature parameter selection - an interpreter level detail rarely discussed in the literature - on fracture density prediction.

The Falher F tight sandstone of the deep basin in Alberta, Canada, is gas charged, deeply buried at about 3,200 meters true vertical depth, and over-pressured with gradients of about 14.5 kilopascals per meter. The net horizontal stress in the Falher F is quite low, which makes the drilling mud window narrow. Compounding this operational challenge is the fact that the sand has abundant natural fractures, which can lead to mud losses or gas kicks depending on the management of the mud weight. Either the loss of too much mud or the uncontrolled production of too much gas can lead to catastrophic operational failure in this over-pressured system.

Case Study

We assessed the best curvature parameterization as being the one in which the hazard presented by the natural fractures was most clearly interpreted from map and line views, and had the highest correlation to fracture density. We argue that the interpretive objective, or target, should generally be given primary consideration when choosing curvature parameters. Our study area is depicted in Figure 1, and has four horizontal wells, depicted as wells 0, A, B, and C. Well 0 and Well A both encountered numerous open fractures, suffered uncontrolled losses of drilling mud and were abandoned due to related operational concerns. Well C had no discernable operational issues, although some fracture infill material was reported by the wellsite team. The operational failure of wells 0 and A suggest that a high density of fractures must exist near the end of those wellbores. Well B has image log fracture density data, which is displayed in Figure 1a. Figure 1b shows a larger area around the wells with two evaluation lines displayed in white. The lower seismic line is depicted in Figure 1c. A reasonable but uncertain interpretation of the events from these wells is that a trend of high density fractures exists in a curve or line going from the toe of Well 0, past the high fracture density area of Well B, to the toe of Well A. The lateral length of Well B is just over 1,500 meters. Exact scales and the direction of North are not given to protect the confidentiality of the data.

Method

While an interpreter defines surface patches of a given size (xy) and appropriate software algorithms then fit with a mathematical quadratic surface, second-order derivatives are estimated from a cuboid of data (xyz) for volumes. Different curvature measures are then computed from the coefficients of the quadratic surface or second-order derivative measures. For a more detailed description of how surface and volumetric curvature attributes are estimated from seismic data, please see Mapping Geologic Features Using Seismic Curvature, Search and Discovery Article #40272.

As the most-positive and most-negative curvature attributes are found to be the easiest measure to visually correlate to the features of geologic interest, a series of most-positive curvature were created on structure-oriented filtered seismic data. The estimates of most-positive curvature using different methods varied by their parameters and are described by:

• Whether the estimates are based on horizon or volumetric estimation methods.

• The size of the cuboid that is used in the initial estimate of the derivatives (x- and y-size are in traces, z-size is in milliseconds).

• The type of filtering applied to the curvature values, which is workflow dependent. This refers to unfiltered curvature estimates, Gaussian filtering or Fourier filtering.

The estimates of the most-positive curvature were derived from four separate industrially offered applications. The Gaussian size is given only by two numbers, the first defining a proxy for the x- and y-size, and the second number defining the z-size. Qualitative comparisons were made based on the map interpretation of curvature and the two lines described in Figure 1. Quantitative evaluation of curvature was made by linear regression with the upscaled fracture density from the image log of the 1,500-meter long lateral of Well B.

Results

Only a small subset of the results is shown in this article though the comparison was carried out on both vertical lines as well as horizontal displays from the attribute volumes.

Figure 2 depicts a subset of the map comparisons. The image log fracture density as shown along the lateral of Well B along with the position of the toe of Wells 0 and Well A are important considerations in this figure, as interpretability was based on the expected arcuate or linear curvature feature connecting the toes of Well 0, Well A, and the high fracture densities from Well B. All the results, except for the horizon-based one, show the expected high most-positive curvature trend, although some details change in the complexity of the trend. The horizon based map of Figure 2a was considered poor as it was dominated by pick-based artefacts (enclosed in a circle). The main arcuate feature mentioned above is shown in black dashed curve and overlaid on the images in (b) to (d). The unfiltered 9x9x98 milliseconds volumetric result of Figure 2b appears quite interpretable on map view, although smaller time (z) windows gave poor results. The Gaussian filtered volumetric result is shown in Figure 2c, and is considered good. The Fourier filtered result (with a fractional index parameter alpha=0.2) is shown in Figure 2d, and is considered excellent, especially in its preservation of curved features.

Linear regression was performed between the most-positive curvature maps and the fracture densities from the image log along the lateral of Well B. Figure 3 shows the log comparison, the correlation coefficients, and rolls up the overall evaluation of the parameter test. Figure 3a shows the correlations of curvature and fracture density in a log format. The entire set of results is summarized in Figure 3b. The Fourier filtered results were the most robust to parameterization and were stable at small cuboid sizes. The Gaussian filtered results seemed decent for all but the smallest and largest parameters tested.

The unfiltered volumetric approach required large time windows, which was concerning to the localization of the interpretation for fractures. The horizon-based method suffered from pick based artefacts in most comparisons.

Conclusions

The interpretation of the distribution and density of natural fractures was affected by the curvature parameters. The volume-based approaches seemed better in map evaluation than the horizon-based estimates, although the smallest xyz cuboid size of the volumetric estimates tended to bear greater similarity to the horizon solutions. Filtering of the curvature results was also material to the evaluation of the risk from natural fractures, with the Fourier based filtering showing the most robustness to different parameterization. Of the volume-based methods, the unfiltered approach was most problematic to effective interpretation, requiring bigger time windows for stability. Evaluation of the best parameterization of curvature required the use of objective correlations to the interpretive target as well as more subjective map and line comparisons. Based on the interpretation of fractures, there appeared to be a sweet spot size for the cuboid or filtering for each of the volumetric approaches. A rational approach to choosing the parameters for curvature requires the consideration of the interpretive objective or target, as “best” is inextricably bound by purpose.

Acknowledgements

Seismic data is owned or controlled by Seismic Exchange, Inc.; interpretation is that of Jupiter Resources Inc. We thank SEI Canada for permission to show certain images of data licensed from them.

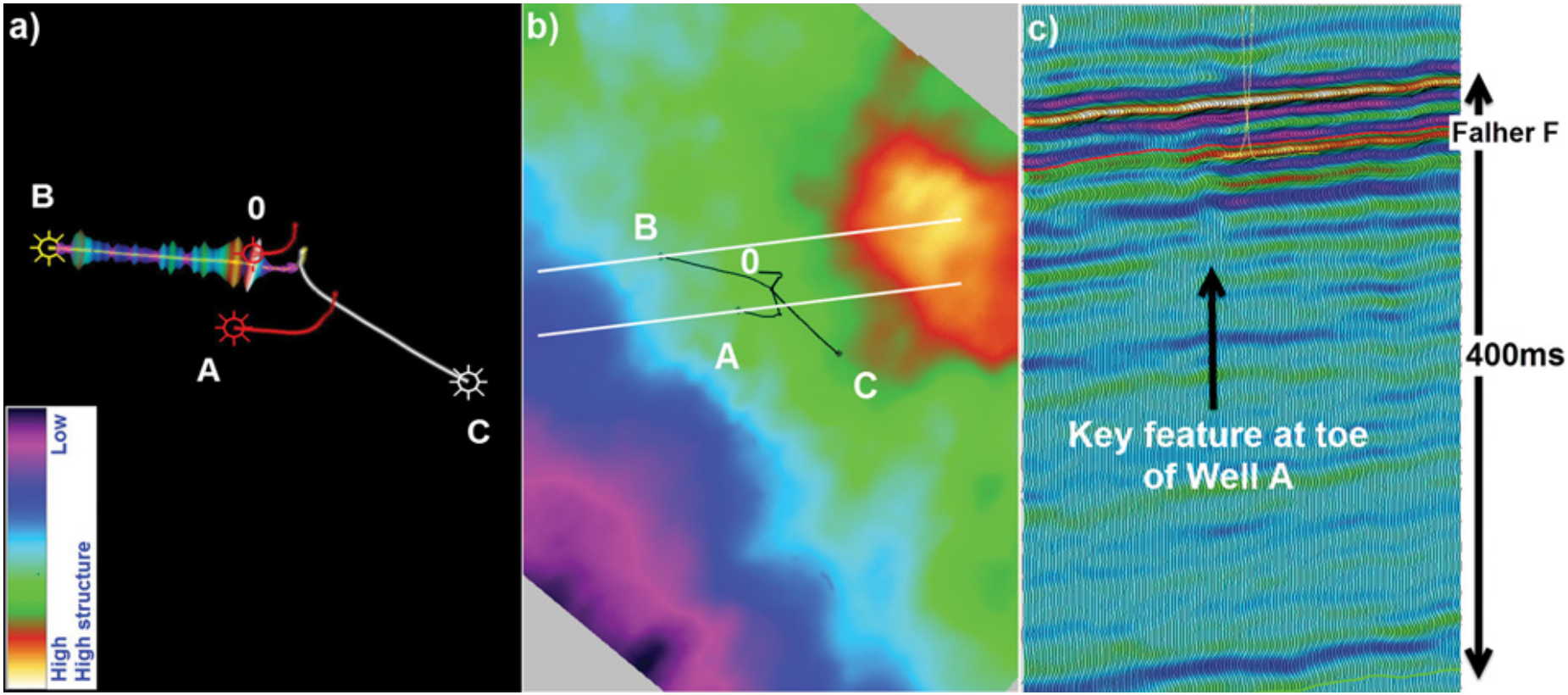

Figure 1. Maps depicting the key elements of the case study. (a) A 3-D perspective view of wells 0, A, B, and C. Well B has an image log estimate of fracture density. The fracture density is displayed as rings whose size is linearly proportional to density. Well 0 and Well A both encountered numerous open fractures, suffered uncontrolled losses of drilling mud and were abandoned due to related operational concerns. Well C had no discernable operational issues, although some fracture infill material was reported by the wellsite team. (b) A time structure map of the Falher F for a portion of the study area. The two seismic lines to be used in the line analysis are shown as the white straight lines. (c) The southernmost of the two indicated seismic lines. The toe of Well A is indicated by an arrow, and coincides with a structural feature. All seismic data images are arbitrarily cut and rotated, with exact scales hidden, to protect the confidential nature of the data. The same color bar is used for all the images.

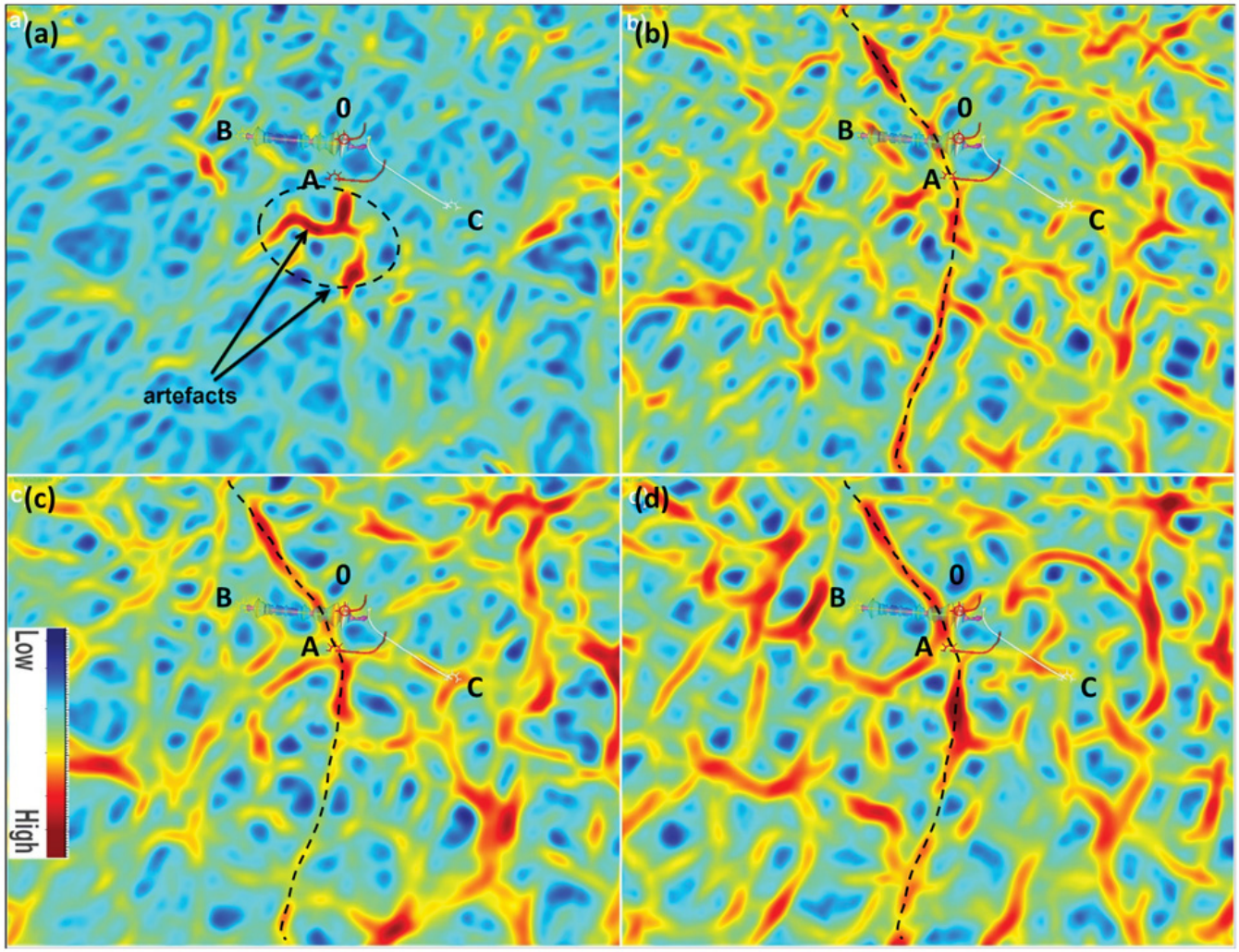

Figure 2. Most-positive curvature attribute estimates at the Falher F surface. Image log fracture density data along Well B are shown as discs proportional in size to the fracture density. (a) The 9x9 horizon based method has artefacts (shown enclosed in a circle) which are the dominant feature of the image. The expected arcuate feature connecting the toes of Well 0, Well A, and the high fracture densities from Well B is shown with a black dashed curve on images (b) to (d). (b) The 9x9x98 ms, unfiltered volumetric method appears reasonable. Shorter time windows appeared unstable and were more difficult to interpret. (c) The 2x9 Gaussian filtered volumetric method is not materially dissimilar to the unfiltered result. The Gaussian size has a complex definition. (d) The 5x5x22 ms Fourier filtered with an alpha value of 0.2 has better preservation of curved features in map view, which may be implementation related.

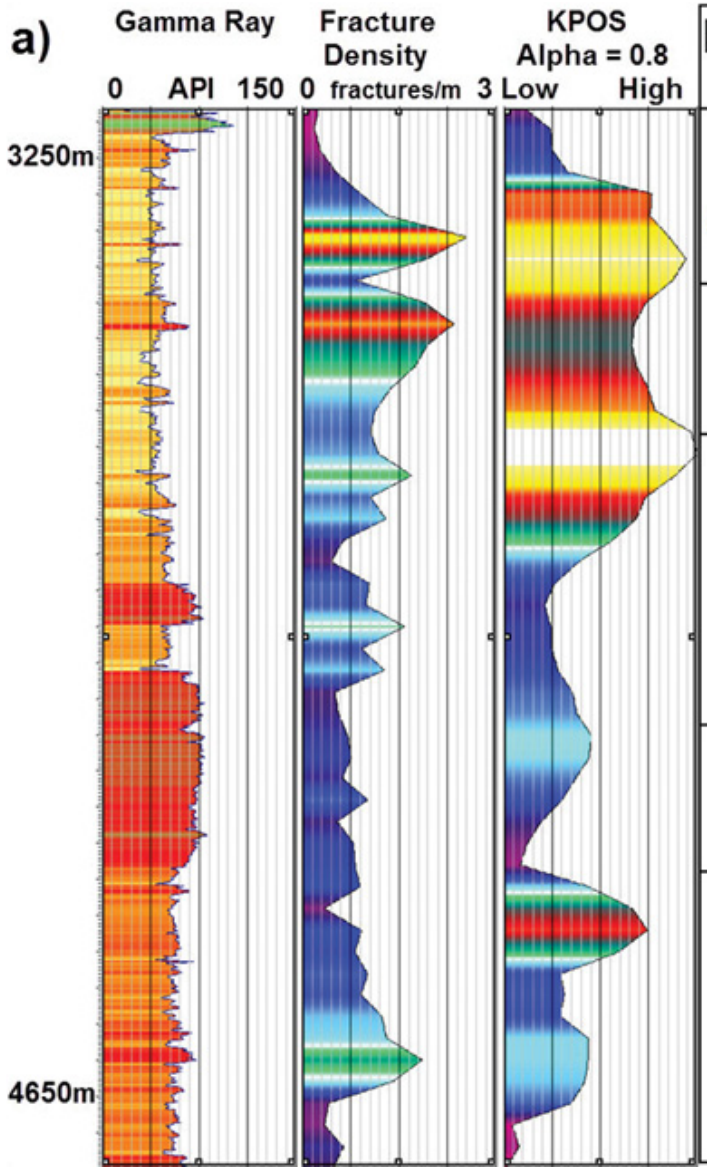

b) Description of Curvature Algorithm and Parameters		Correlation Coefficients	Qualitative Evaluation	
Type of Algorithm	Parameters - all KPOS	With Fracture Density, 55 samples	Map Response	Line Response
Horizon based	7x7 Grid	.408	artefacts	not applicable
	9x9 Grid	.402	artefacts	
	15x15 Grid	.371	artefacts	
	17x17 Grid	.375	ok?	
Linear weighted cuboid (Unfiltered)	3x3x98	-.104	unuseable	unuseable
	5x5x98	-.045	poor	poor
	7x7x98	.168	good-noisy	good-noisy
	9x9x22	.100	poor	poor
	9x9x46	.185	poor	poor
	9x9x98	.263	good	good
	11x11x98	.295	good	good
	17x17x98	.308	degrading	degrading
Gaussian weighted cuboid	1x5	.516	poor	poor
	2x9	.527	good	good
	3x10	.515	good	good
	5x10	.483	degrading	degrading
Fourier filtered 5x5x22ms cuboid	Alpha 0.8	.597	degraded?	degraded?
	Alpha 0.65	.565	good	good
	Alpha 0.5	.375	good	good
	Alpha 0.4	.375	good	good
	Alpha 0.2	.509	good	good
	Alpha 0.2 50ms window	.439	degraded	degraded
	Alpha 0.4 50ms window	.415	degraded	degraded
	Alpha 0.8 50ms window	.390	degraded	degraded

Figure 3. Selected results. (a) Gamma Ray log, upscaled fracture density from image log data, and most positive curvature with Fourier filtering and an alpha value of 0.8 for the horizontal length of Well B. (b) A results summary with a roll-up of the correlations to fracture density as well as the qualitative line and map based evaluations. Correlation coefficients passing the 1 percent p-test for significance are colored dark yellow.